4-15-1991

Reconstructions of Au films on Pd(110)

P. J. Schmitz
Iowa State University

W.-Y. Leung
Iowa State University

H.-C. Kang
Iowa State University

Patricia A. Thiel
Iowa State University, thiel@ameslab.gov

Reconstructions of Au films on Pd(110)

Abstract
We present a study of thermally activated changes in Au films, 1–10 monolayers thick, on Pd(110). The films are stable against bulk dissolution until ~500 K, based upon Auger electron spectroscopy. For Au coverages below 1.5 monolayers, only a (1×1) overlayer structure is observed with low-energy electron diffraction over the entire temperature range studied (130–800 K). At coverages above 1.0 monolayers and after annealing to temperatures above 300 K, a (1×z) diffraction pattern develops. With increasing coverage the value of z increases continuously from 2 to 3, reaching z=3 at 4 monolayers. We propose that the diffraction pattern reflects a coverage-dependent mixture of small domains of (1×2) and (1×3) reconstruction, with the (1×2) favored at low coverage and the (1×3) favored at high coverage. This model is rationalized in terms of the film's coverage-dependent morphology, which can be described as Stranski-Krastanov with a critical thickness of 2 monolayers.

Keywords
Ames Laboratory

Disciplines
Physical Chemistry

Comments
This article is from *Physical Review B* 43, no. 11 (1991): 8834–8840, doi:10.1103/PhysRevB.43.8834.

Reconstructions of Au films on Pd(110)

P. J. Schmitz,* W.-Y. Leung,† H. C. Kang, and P. A. Thiel
Department of Chemistry and Ames Laboratory, Iowa State University, Ames, Iowa 50011
(Received 19 October 1990)

We present a study of thermally activated changes in Au films, 1–10 monolayers thick, on Pd(110). The films are stable against bulk dissolution until ~500 K, based upon Auger electron spectroscopy. For Au coverages below 1.5 monolayers, only a (1×1) overlayer structure is observed with low-energy electron diffraction over the entire temperature range studied (130–800 K). At coverages above 1.0 monolayers and after annealing to temperatures above 300 K, a $(1\times z)$ diffraction pattern develops. With increasing coverage the value of z increases continuously from 2 to 3, reaching $z=3$ at 4 monolayers. We propose that the diffraction pattern reflects a coverage-dependent mixture of small domains of (1×2) and (1×3) reconstruction, with the (1×2) favored at low coverage and the (1×3) favored at high coverage. This model is rationalized in terms of the film's coverage-dependent morphology, which can be described as Stranski-Krastanov with a critical thickness of 2 monolayers.

I. INTRODUCTION

The (110) faces of Au, Pt, and Ir are known to exhibit $(1\times n)$ "missing-row" reconstructions, where n can take the values of 2 and 3, and even higher integers (e.g., see Refs. 1–24). It is the objective of this study to determine whether and under what conditions Au films may reconstruct when grown on the (110) face of another fcc metal which does not reconstruct, Pd.[25,26] For the clean (110) surface of bulk Au, (1×2) reconstructions are most frequently reported in the literature,[1–12] but (1×3) structures have also been reported.[10–12] We observe both of these structures for the Au films, their formation depending directly on the film thickness and annealing temperature.

In a previous paper, we described the growth mode and CO chemisorption properties of Au/Pd(110) grown at 130 K. We concluded that the films obey Stranski-Krastanov growth with a critical thickness of two monolayers, i.e., sequential population of the first two monolayers is followed by three-dimensional agglomeration.[27] Presumably, the transition from two-dimensional to three-dimensional growth is caused by the 4.8% lattice mismatch between Au and Pd, which induces a coverage-dependent strain energy. In the present paper, we relate the coverage-dependent morphology to the coverage-dependent reconstructions exhibited by the Au film.

II. EXPERIMENTAL PROCEDURES

Most of the experimental procedures are described elsewhere.[27] In brief, the experiments take place in an ultrahigh-vacuum system equipped for Auger electron spectroscopy (AES), mass spectrometry, ion bombardment, low-energy electron diffraction (LEED), and Au evaporation. The relative Au coverage, following evaporation, is determined using AES. The relationship between this measure of *relative* coverage and the *absolute* coverage is presented elsewhere.[27] [An absolute coverage Θ of one monolayer (ML) is herein defined as one adatom per surface Pd atom, or 9.35×10^{14} atoms cm^{-2}.] The Au deposition rate is on the order of 10^{-2} ML s^{-1}. Depositions at substrate temperatures of 130 and 300 K reveal no difference in the resulting overlayer superstructures. This paper presents only experiments in which the film is initially prepared via deposition at 130 K.

In the annealing sequences, the crystal is heated to a specified temperature, held for 20 s, then cooled below 200 K where the LEED or AES data are acquired. Therefore only irreversible changes are detected. The diffraction pattern is recorded via a silicon-intensified-target camera on a video tape, and later processed with a computerized image-acquisition system.[28] The LEED intensity profiles are measured along the [001] direction, i.e., between the reciprocal-space (1,0) and (1,−1) positions. Diffuse intensity elongated between these two reciprocal-space positions is referred to as streaking. The incident electron beam energy is 72 eV and the crystal current is 70 nA.

III. EXPERIMENTAL RESULTS

For $\Theta_{Au}\leq1$, a simple (1×1) diffraction pattern is observed, with no fractional-order spots or streaking detectable at any temperature. At $\Theta_{Au}>1$, fractional-order beams appear, reach maximum intensity, then disappear as the film is progressively annealed. These trends are evident in the spot profiles of Fig. 1. At a coverage of 1.5 ML [Fig. 1(a)], a $(1\times z)$ superstructure forms irreversibly above 300 K, becomes most intense at 530 K, and then fades at higher temperature. The superstructure spots are very close to the half-order position, although a small splitting about the half-order position is visible after annealing to 310 K. At higher temperature, this splitting disappears and $z=2$. At 2 ML [Fig. 1(b)], a half-order spot again develops above room temperature, with some splitting about the half-order position, then coalesces into

a bright (1×2) at 640 K. By 770 K, the (1×2) is lost.

At higher coverage, the half-order spots split continuously toward the integral-order spots until 4 ML, when the third-order positions are gained. This splitting is mainly a function of coverage, not of temperature, as shown in Figs. 1(c), 1(d), and 1(e) ($\Theta_{Au}=3$, 4, and 5). Figure 2 shows the maximum value of $\Delta k_{\parallel}$ versus Θ_{Au} for the fractional-order component. The spot moves continuously from the half-order to the third-order position (indicated by the dashed line) as Au coverage increases from 1.5 to 4 ML.

In the coverage regime $\Theta_{Au}\geq 2$, heating to 640 K always causes the split spots to remerge to half-order positions. The resultant (1×2) pattern then remains, up to 740 K; above 740 K, the (1×1) is regained. At $\Theta_{Au}=6$ [Fig. 1(f)], the fractional-order beams are barely visible above background, and even the integral-order spots are very weak. At $\Theta_{Au}\geq 7$ and at temperatures where the (1×3) has transformed to the (1×2) (i.e., $T\geq 640$ K), the faint and streaky (1×2) is accompanied by weak satellites around the integral-order and fractional-order beams, in the [1$\bar{1}$0] direction. Although we have not investigated the latter effect in detail, it may indicate growth of pyramidal or wedge-shaped clusters such as those described for Ag/Cu(110).[29]

Table I summarizes the structural transitions which occur in the Au film, at various coverages and temperatures. All of the structural transitions reported here are irreversible. An explanation can be found in the temperature dependence of the film and substrate Auger intensities. These data are displayed in Fig. 3 as the Au/Pd

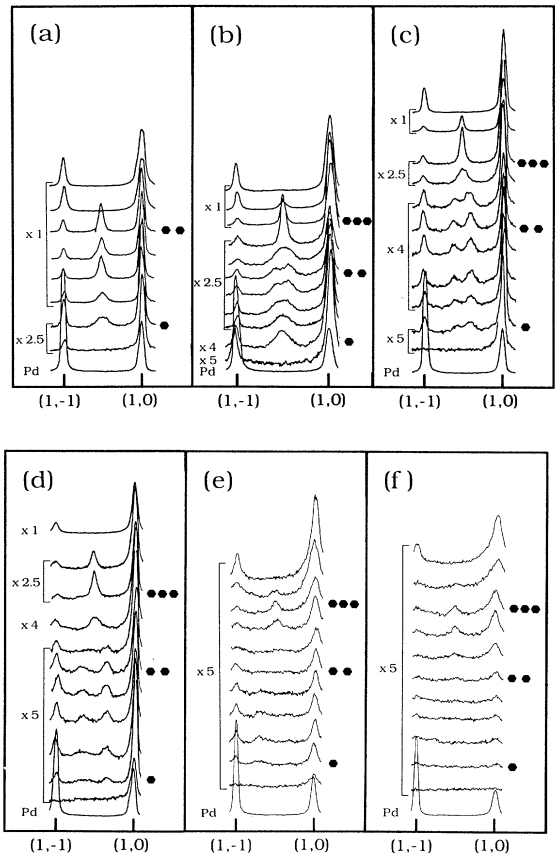

FIG. 1. LEED profiles for various Au coverages on Pd(110) as a function of annealing temperature. Intensity scaling factors are given relative to the clean Pd substrate at 130 K. The curves at 310, 530, and 690 K are always marked with one, two, and three dark symbols, respectively. (a) $\Theta_{Au}=1.5$. The sequence of annealing temperatures (in K) from bottom to top is 130 (clean), 130 (with Au), 310, 340 , 410, 470, 530, 580, and 640. (b) $\Theta_{Au}=2$. The sequence of annealing temperatures (in K) from bottom to top is 130 (clean), 130 (with Au), 310, 340, 410, 470, 530, 580, 640, 690, 740, and 770. The annealing sequence for panels (c)–(f) is identical. (c) $\Theta_{Au}=3$. (d) $\Theta_{Au}=4$. (e) $\Theta_{Au}=5$. (f) $\Theta_{Au}=6$.

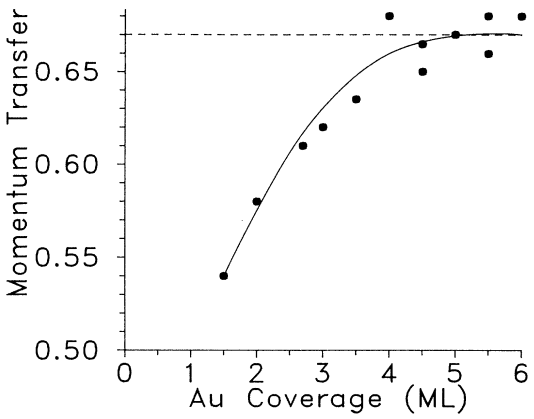

FIG. 2. Variation of the maximum $\Delta k_{\parallel}$ (in Å^{-1}) for the fractional-order LEED spot as a function of Au coverage. The splitting shown is that measured after annealing to 530 K, except for the 1.5-ML film, where the measurement is made after a 310-K anneal. The solid line is drawn only to guide the eye.

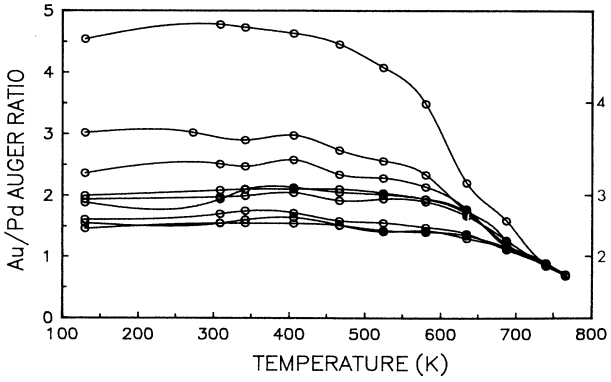

FIG. 3. Variation of the $Au_{69}(NVV)$ to $Pd_{330}(MNN)$ Auger peak ratio vs annealing temperature. The right-hand axis is labeled with selected values of *initial* gold coverage.

TABLE I. Temperature-dependent progression of superstructures observed for the Au films, in three major coverage regimes.

Coverage regime	Structural sequence with increasing temperature
$\Theta_{Au} < 1.5$	(1×1)
$\Theta_{Au} \approx 1.5$	$(1\times1) \xrightarrow{310\ K} (1\times z)^a \xrightarrow{530\ K} (1\times1)$
$2 \leq \Theta_{Au} < 7$	$(1\times1) \xrightarrow{310\ K} (1\times z)^a \xrightarrow{640\ K} (1\times2) \xrightarrow{770\ K} (1\times1)$

[a]z varies smoothly from 2 to 3 with increasing Θ_{Au}, as shown in Fig. 2.

Auger intensity ratio versus temperature. At temperatures in excess of 500 K, the intensity ratio decreases for all the Au films. This decrease may be due to loss of Au via dissolution of the overlayer into the Pd substrate. Alternatively, it could be due to thermally activated three-dimensional agglomeration as has been observed, for instance, for Pd/W(110).[30] We favor the former explanation, since Au and Pd are known to form a continuous series of solid solutions.[31] Furthermore, our previous study has suggested that the Au film agglomerates above the critical coverage of 2 ML, *even at temperatures as low as 130 K*. Therefore simple diffusion-mediated aggregation must be associated with a relatively low energetic barrier. The transitions which the films undergo at $T \geq 500$ K are associated with a higher activation barrier, implying a fundamentally different process. We propose that this process is intermixing between substrate and film, accompanied by effective reduction of the film coverage.

Information is also contained in the coverage and temperature dependence of the superstructure intensity. Figure 4 depicts the intensity variation with *coverage,* i.e., the height of the fractional-order component at $T=530$ and 690 K as a function of Au coverage. [The component closest to the (1,0) spot is arbitrarily but consistently chosen for this measurement.] It is apparent that annealing produces the brightest spots when the film is 1.5 or 2 layers thick; the superstructure dims substantially at higher Au coverages, for a fixed annealing temperature. Figure 5 depicts the intensity variation with *temperature,* for various Au coverages. This representation shows that the superstructure brightens just before it disappears, at all coverages, and that its subsequent disappearance at high temperature is abrupt. The intensification always corresponds to the conversion from $(1\times z)$ to (1×2) superstructures described in Table I.

IV. DISCUSSION

A. Origins of (1×2), (1×3), and $(1\times z)$

The (1×2), (1×3), and intermediate $(1\times z)$ superstructures observed with LEED could reasonably be assigned to one of two classes. The first is a bulklike reconstruction of the Au film. This assignment is supported by previous observations both of (1×2) and (1×3) reconstructions for the clean (110) surface of bulk Au.[1–12] The

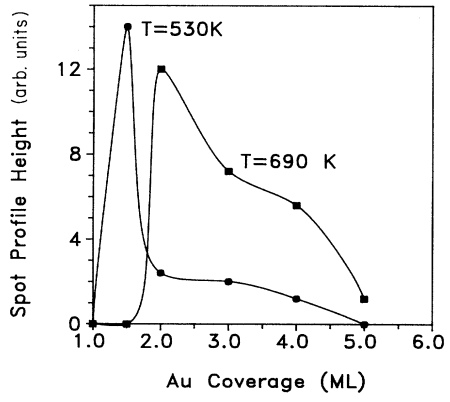

FIG. 4. Height of the fractional-order LEED spot profile as a function of Au coverage. Circles represent intensities obtained after annealing to 530 K, where a good $(1\times z)$ pattern is obtained $(2 \leq z \leq 3)$. Squares represent intensities obtained after annealing to 690 K, where the (1×2) is restored. See Table I for clarification of the coverage- and temperature-dependent progression of LEED patterns. Solid lines are drawn only to guide the eye.

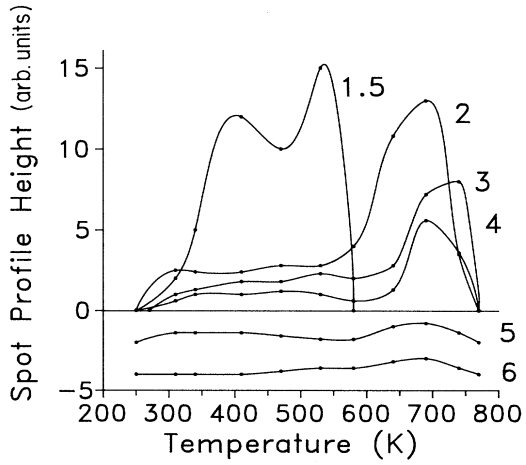

FIG. 5. Height of the fractional-order LEED spot profile as a function of annealing temperature. Each curve is labeled with the Au coverage in ML. The curves for 5 and 6 ML are displaced vertically by values of −2 and −4, respectively, for clarity. Solid lines are drawn only to guide the eye.

second plausible assignment is an ordered surface alloy of Au and Pd. This suggestion is supported by the bulk phase diagram for the Au-Pd system, which shows regions of ordered alloys.[31] The hypothesis of a stoichiometric Au-Pd surface alloy is also supported by the fact that the brightest (1×2) LEED patterns are usually obtained above 600 K (Fig. 5), i.e., well above the temperature at which AES shows loss of Au. However, the (1×z) and (1×3) patterns *first* emerge by 310 K, which is well *below* the temperature at which dissolution starts. Therefore the ordered-alloy hypothesis can be excluded for the (1×z) and (1×3) patterns produced at low temperature, but it cannot be ruled out for the bright (1×2), which develops with high-temperature annealing.

We support the hypothesis that all of the superstructures are bulklike reconstructions, largely by analogy with our studies of Pt films on Pd(110), where (1×2) and (1×3) superstructures also form.[32] For the Pt/Pd system we have shown that the (1×z) superstructures reversibly interchange with the (1×1) structure, upon adsorption and desorption of CO. While it is known that CO adsorption can "lift" the reconstructions of bulk Pt(110),[19,33] it is unlikely that CO adsorption could disorder a surface alloy. Furthermore, analysis of the intensity-energy profiles of the (1×2) LEED pattern for the Pt/Pd(110) system shows that best agreement is obtained for a bulklike reconstruction of the Pt film.[34] Thus, by analogy, we support assignment of the (1×z) superstructures to bulklike reconstructions in the Au film. Some type of structural analysis must be applied to the Au/Pd(110) system as well, however, before the assignment can be made with complete certainty.

Possible models for the reconstructions of clean (110) surfaces of *bulk* Au are shown in Fig. 6. Analogous

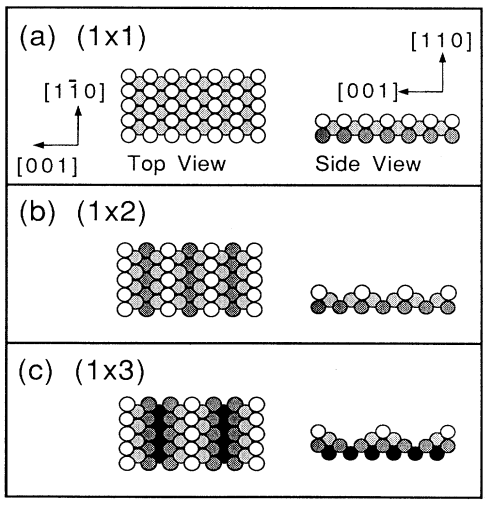

FIG. 6. Schematic representation of the (110) "missing-row" reconstructions. Open circles represent atoms in the surface layer; progressively darker shading represents atoms in progressively deeper layers. (a) (1×1) (unreconstructed). (b) (1×2). (c) (1×3).

reconstructions are displayed also by Pt(110) and Ir(110). The (1×2) structure of Fig. 6(b), with one missing row per unit cell, is well established (e.g., see Refs. 10, 14, and 15). The less-common (1×3) structure is also assigned to a missing-row structure, as shown in Fig. 6(c).[15,21] In the (1×3), there are three missing rows per (1×3) unit cell, two in the first layer and one in the second layer. Thus the troughs (facets) are deeper in the (1×3) structure than in the (1×2). In going from the (1×1) to the (1×2) or (1×3), it is necessary that some of the rows "disappear." Scanning tunneling microscopy has shown that the mechanism of this mass transport is the creation of new terraces or growth of existing terraces.[35] Heating the Au films above room temperature is almost certainly necessary to form the (1×z) reconstructions because of the activation barrier associated with this mass transport.

B. Coverage-dependent development of LEED patterns

First, we discuss the fractional-order spots observed at temperatures *below* emergence of the bright (1×2). Figure 2 shows that z_{max} varies smoothly from 2 to 3 as coverage increases from 1.5 to 4. We propose that this is due to coexistence of (1×2) and (1×3) domains which are smaller than the transfer width of our LEED optics (~100 Å). As coverage increases, the fractional surface area contributing to the diffraction pattern *and* covered by (1×3) domains increases, while the fraction covered by (1×2) domains falls. Similar phenomena have been observed in chemisorption systems, for instance, for the lattice-gas system O/Pd(110),[36,37] and for the adsorbate-induced reconstruction of O/Ni(110).[38] However, to our knowledge, this is the first observation of continuous splitting in reconstruction of a clean metal surface, film or bulk.

In our system, the question is the following: Why is the (1×3) favored by high Au coverages? This is particularly puzzling since the (1×2) is the reconstruction most often reported for (110) surfaces of *bulk* Au, Pt, and Ir. With increasing Au coverage, one would expect the film to approach bulk properties, contrary to this observation. In a previous paper, we have proposed that Au films grow on Pd(110) in Stranski-Krastanov (SK) fashion with a critical coverage of 2 ML.[27] That is, the films grow layer by layer up to 2 ML, then grow as three-dimensional clusters. We believe that the reconstructions are related to this growth mode and, particularly, to the surface roughness which develops above 2 ML.

Part of our model hinges upon the fact that the facets in the (1×2) reconstruction are probably more shallow than in the (1×3). Thus it is reasonable that the minimum local thickness required to support the (1×2) reconstruction is lower than that required for the (1×3). We first observe the (1×2) reconstruction at $\Theta_{Au}=1.5$, where half the surface is covered by a two-layer film. This suggests that the minimum local thickness for the (1×2) is 2 ML. Figure 6(b) reveals that reconstruction at this coverage would leave only Au atoms exposed at the vacuum interface, except for the Pd atoms at the very bottom of the troughs. At the same time, the "missing" rows could migrate to adjacent areas where the Au is

only one layer deep, and create additional (1×2). Even at this coverage, however, there is some splitting due to a small contribution from (1×3) areas, suggesting that the two-layer film is not spatially uniform.

Note also that the (1×2) pattern formed at this coverage is much brighter than the superstructures formed at higher coverage, for instance at 530 K (cf. Fig. 5). This demonstrates that the progression from (1×2) to (1×3) superstructures with increasing coverage is accompanied by a decrease in the number of scatterers from which these patterns originate.

At $\Theta_{Au} > 1.5$, the contribution of the (1×3) increases at the expense of the (1×2), until third-order spot positions are reached at 4 ML. This may be due in part to the simple fact that, as Θ_{Au} increases, areas of the Au film grow deep enough to support the (1×3) reconstruction—which, by analogy with the (1×2), would require a local depth of three layers [cf. Fig. 6(c)]. However, this alone is not sufficient to explain the intensity variation with coverage shown, e.g., in Fig. 5, as well as the fact that the (1×3) is not the preferred reconstruction of bulk Au(110) under these conditions. Therefore we postulate that film morphology controls the transition from the (1×2) to (1×3) reconstruction with increasing coverage. Our model is shown in Fig. 7. As three-dimensional clusters develop, they occupy increasing surface area. They do not contribute directly to the superstructure pattern, but they serve to break up the contiguous areas of smooth, two-layer film, where the (1×2) reconstruction is preferred. Further, we propose that the perimeters of the clusters are microscopically rough, and serve to nucleate and/or stabilize the (1×3) on the adjoining terraces. However, as the clusters grow larger the smooth terraces shrink, and even the fractional area covered by (1×3) reconstruction eventually goes to zero. Thus the brightness of the superstructure pattern decreases with increasing coverage as shown in Fig. 5, and at the same time the diffraction pattern converts continuously from (1×2) to (1×3). The idea that the perimeters of the clusters serve to nucleate and/or stabilize (1×3) regions is supported by the fact that (110) surfaces of bulk Pt, Ir, and Au most often exhibit the (1×3) reconstruction under conditions where the surface smoothness or cleanliness are somewhat suspect (see, e.g., Ref. 15).

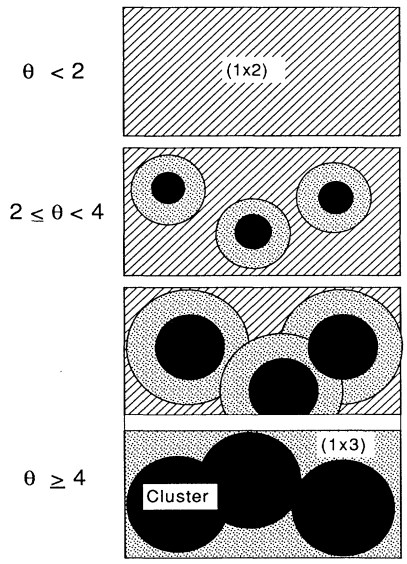

FIG. 7. Schematic representation of the model for coverage-dependent changes in Au film structure.

In a morphologically similar system, Au/Ag(110), Fenter and Gustafsson have also observed (1×2) and (1×3) superstructures.[39] However, the coverages necessary to produce these patterns are much higher than we observe for Au/Pd(110). There are other important differences as well, such as the sequence in which the (1×2) and (1×3) appear with increasing coverage. [They observe that the (1×3) *precedes* the (1×2) as coverage increases; we find the opposite.] The relationship between the phenomena observed in their system, and in ours, is intriguing but unclear.

C. Effect of dissolution

It is interesting to note that the variation of superstructure *intensity* with temperature at fixed initial Θ_{Au} (Fig. 5) is almost a mirror image of its variation with increasing Θ_{Au}, at fixed annealing temperature (Fig. 4). A similar reversal is also displayed in the variation of superstructure *periodicity* with temperature and coverage. With increasing temperature at fixed initial coverage, the system progresses from a (1×z) to a (1×2) (Fig. 1), whereas with increasing coverage at fixed annealing temperature, the opposite progression can be followed—from (1×2) to (1×z) (Fig. 2). This reversibility suggests that the major effect of annealing and dissolution is simply to cause a decrease in film coverage.

For instance, in Fig. 6, at $\Theta_{Au}=3$, annealing above room temperature brings on the faint (1×z) structure, where z is intermediate between 2 and 3. However, upon annealing above 640 K, the intensity abruptly rises; Fig. 1 shows that this corresponds to the return of the (1×2) structure. The AES data of Fig. 3 show that dissolution of Au accompanies these changes, and we propose that at about 640 K dissolution has reduced the *effective* Θ_{Au} to 1.5–2 ML. [By speaking of an effective coverage, we acknowledge that the concentration gradient of Au in the bulk has an unknown effect on the properties of the surface layer(s), and specifically on the absolute coverages required to achieve certain reconstructions, under these conditions.] Thus the film becomes smooth, the (1×3) is destabilized, and large (1×2) domains replace it. Above 740 K, the effective Θ_{Au} drops below 1.5–2 ML, and the LEED pattern reverts abruptly to the (1×1). Figure 3 confirms that massive dissolution has occurred by this temperature.

It must be noted that the thermal variation of superstructure intensity at 1.5 ML diverges significantly from the pattern established at other coverages. Not only is the superstructure more intense, but reversion to (1×1)

occurs at much lower temperature, 530 K. Perhaps this reflects a relatively low stability against thermal dissolution at $\Theta_{Au} < 2$. Unfortunately, the AES data are not adequate to support or disprove this possibility.

V. CONCLUSIONS

The major results of this work can be summarized as follows.

(i) Au films on Pd(110) exhibit (1×2), (1×3), and intermediate $(1\times z)$ superstructures upon annealing between 300 and 800 K. We propose that these represent bulklike missing-row reconstructions, whose formation is thermally activated. The intermediate $(1\times z)$ superlattice is then a mixture of small domains of (1×2) and (1×3).

(ii) The minimum total coverage required for the (1×2) is 1.5 ML. At lower coverage, there is no evidence of superstructures. We propose that the depth of the facets in the (1×2) reconstruction is such that a local thickness of 2 ML is necessary to support it.

(iii) As Θ_{Au} increases from 1.5 to 6, the $(1\times z)$ superstructure becomes increasingly faint. Simultaneously, the value of z changes smoothly from 2 to 3. We attribute this to a coverage-dependent mixture of small (1×2) and (1×3) domains, with the (1×3) favored by higher Θ_{Au}. The coverage dependence may spring from the SK growth mode, where three-dimensional clustering occurs above 2 ML. The clusters deplete the surface area available for reconstruction, and favor the (1×3) over the (1×2) by enhancing surface roughness.

(iv) The (1×2) pattern is regained, and the superstructure intensity is enhanced, by annealing above 640 K. This probably occurs because dissolution brings the effective surface coverage of Au down to 1.5–2 ML, at which point the three-dimensional clusters are no longer stable. However, it is also possible that an ordered (1×2) surface alloy forms under these conditions.

ACKNOWLEDGMENTS

We thank R. J. Baird and G. W. Graham of Ford Motor Company for the use of their Pd(110) crystal. This work was begun with support from the National Science Foundation under Grant No. CHE-8451317 and continues via Grant No. CHE-9014214. It is also supported by the Camille and Henry Dreyfus Foundation, and by the Ford Motor Company. One of us (P.J.S.) acknowledges the support of the Phillips Petroleum Corporation. In addition, some equipment and all facilities are provided by the Ames Laboratory, which is operated for the U.S. Department of Energy by Iowa State University under Contract No. W-7405-ENG-82.

*Present address: Ford Motor Company, Dearborn, MI 48121.
†Present address: Department of Physics, Florida International University, Miami, FL 33199.

[1]D. G. Fedak and N. A. Gjostein, Acta Metall. **15**, 827 (1967).
[2]D. Wolf, H. Jagadzinski, and W. Moritz, Surf. Sci. **77**, 265 (1978).
[3]J. R. Noonan and H. L. Davis, J. Vac. Sci. Technol. **16**, 587 (1979).
[4]I. K. Robinson, Phys. Rev. Lett. **50**, 1145 (1983).
[5]M. Copel and T. Gustafsson, Phys. Rev. Lett. **57**, 723 (1986).
[6]J. Moller, K. J. Snowdon, and W. Heiland, Surf. Sci. **178**, 475 (1986).
[7]K. -M. Ho and K. P. Bohnen, Europhys. Lett. **4**, 345 (1987).
[8]K. -M. Ho and K. P. Bohnen, Phys. Rev. Lett. **59**, 1833 (1987).
[9]P. J. Estrup, in *Chemistry and Physics of Solid Surfaces V*, edited by R. Vanselow and R. Howe (Springer, Berlin, 1984), p. 205.
[10]W. Moritz and D. Wolf, Surf. Sci. **88**, L29 (1979).
[11]G. Binnig, H. Rohrer, Ch. Gerber, and E. Weibel, Surf. Sci. **131**, L379 (1983).
[12]A. Held, J. L. Jordan-Sweet, P. M. Horn, A. Mak, and R. J. Birgeneau, Solid State Commun. **72**, 37 (1989).
[13]M. Salmeron and G. A. Somorjai, Surf. Sci. **91**, 373 (1980).
[14]D. L. Adams, H. B. Nielsen, M. A. Van Hove, and A. Ignatiev, Surf. Sci. **104**, 47 (1981).
[15]P. Fery, W. Moritz, and D. Wolf, Phys. Rev. B **38**, 7275 (1988).
[16]P. Fenter and T. Gustafsson, Phys. Rev. B **38**, 10 197 (1988).
[17]R. Ducros, J. J. Ehrhardt, J. Fusy, and B. Mutaflschiev, Phys. Rev. B **38**, 10 035 (1988).
[18]E. C. Sowa, M. A. Van Hove, and D. L. Adams, Surf. Sci. **199**, 174 (1988).
[19]T. Gritsch, D. Coulman, R. J. Behm, and G. Ertl, Phys. Rev. Lett. **63**, 1086 (1989).
[20]W. Hetterich and W. Heiland, Surf. Sci. **210**, 129 (1989).
[21]M. Shi, H. Bu, and J. W. Rabalais, Phys. Rev. B **42**, 2852 (1990).
[22]M. Shi, H. Bu, and J. W. Rabalais (unpublished).
[23]H. Bu, M. Shi, F. Masson, and J. W. Rabalais, Surf. Sci. Lett. **230**, L140 (1990).
[24]G. L. Kellogg, Phys. Rev. Lett. **55**, 2168 (1985).
[25]M. Wolf, A. Goschnick, J. Loboda-Cackovic, M. Grunze, W. N. Unertl, and J. H. Block, Surf. Sci. **182**, 489 (1987).
[26]R. D. Diehl, M. Lindroos, A. Kearsley, C. J. Barnes, and D. A. King, J. Phys. C **18**, 4069 (1985).
[27]P. J. Schmitz, H. C. Kang, W.-Y. Leung, and P. A. Thiel, Surf. Sci. (to be published).
[28]J. W. Anderegg and P. A. Thiel, J. Vac. Sci. Technol. A **4**, 1367 (1986).
[29]T. N. Taylor, M. A. Hoffbauer, C. J. Maggiore, and J. G. Beery, J. Vac. Sci. Technol. A **5**, 1625 (1987); T. N. Taylor, A. W. Denier van der Gon, and J. F. van der Veen, Phys. Rev. B **41**, 7474 (1989).
[30]W. Schlenk and E. Bauer, Surf. Sci. **93**, 9 (1980).
[31]R. P. Elliot and F. A. Shunk, Bull. Alloy Phase Diagrams **2**, 482 (1982).
[32]P. J. Schmitz, H. C. Kang, W.-Y. Leung, and P. A. Thiel (unpublished); also W.-Y. Leung, P. J. Schmitz, and P. A. Thiel, Vacuum **41**, 471 (1990).
[33]T. E. Jackman, J. A. Davies, D. P. Jackson, W. N. Unertl, and P. R. Norton, Surf. Sci. **120**, 389 (1982).
[34]P. Kaukasdinas, M. Lindroos, H. C. Kang, O. L. Warren, P. J. Schmitz, and P. A. Thiel (unpublished).
[35]D. J. Coulman, J. Wintterlin, R. J. Behm, and G. Ertl, Phys. Rev. Lett. **64**, 1761 (1990).
[36]G. Ertl and J. Küppers, Surf. Sci. **21**, 61 (1970).

[37]G. Ertl and J. Küppers, *Low Energy Electrons and Surface Chemistry* (VCH Verlagsgesellschaft, Weinheim, 1985), p. 241.

[38]L. H. Germer, J. W. May, and R. J. Szostak, Surf. Sci. **8**, 430 (1967).

[39]P. Fenter, Ph.D. thesis, University of Pennsylvania, 1990; P. Fenter and T. Gustafsson, in *The Structure of Surfaces III,* edited by M. A. Van Hove, K. Takayanagi, and X. Xide (Springer-Verlag, Berlin, in press)